

Electronic Supplementary Material (ESI) for ChemComm.

Supporting Information

A facial synthesis of a copper (I) thiourea sulphate complex and its application for highly efficient chalcopyrite solar cells

Shuxia Wei, Chengfeng Ma, Xinge Liu, Naiyun Liu, Mingjun Yuan, Kang Xiao, Weibo Yan* and Hao Xin*

State Key Laboratory of Organic Electronics and Information Displays (SKLOEID), Institute of Advanced Materials (IAM), Nanjing University of Posts & Telecommunications, 9 Wenyuan Road, Nanjing 210023, China.

E-mail: iamwbyan@njupt.edu.cn; iamhxin@njupt.edu.cn

Experimental Methods

Synthesis of copper (I) thiourea sulphate complex

The copper (I) thiourea sulphate complex were prepared as follows: 45.6720g thiourea (TU, 99%, Aladdin) and 29.9475g copper (II) acetate ($\text{Cu}(\text{CH}_3\text{COO})_2 \cdot \text{H}_2\text{O}$, 99%, Aladdin) were dissolved in 100 mL 35°C deionized water. The mixed solution was put into a 35°C water bath pan, stirred at 500 rpm for 2-4 hours. With the reaction, the solution became blurred (Fig. S1a). After complete reaction, the solution was filtered while hot to obtain yellowish green transparent filtrate (Fig. S1b) and yellow solid (Fig. S2). The yellow solid was dried for 12 hours in a vacuum oven at 60°C to obtain a pale-yellow powder (21.9130 g). After the filtration cooled down, white elongated crystals precipitated (Fig. S4). The crystalline precipitates were filtered and washed with anhydrous ethanol and deionized water. The product was dried in a 60°C vacuum oven (Fig. S5). Finally, 26.5175g white crystals were obtained. The pale- yellow powder was named S1, and the white crystal was named S2. (The molar ratio of $\text{Cu}(\text{CH}_3\text{COO})_2 \cdot \text{H}_2\text{O}$:TU was 1:4, the molar concentration of $\text{Cu}(\text{CH}_3\text{COO})_2 \cdot \text{H}_2\text{O}$ was 1.5 mol/L.)

Preparation of the precursor solutions

The solution was prepared in a glove box with H_2O and O_2 levels below 5 ppm. To determine the optimal composition, three solutions with molar ratios of $[\text{Cu}(\text{NH}_2)_2\text{CS}_3]_2\text{SO}_4 \cdot \text{H}_2\text{O}$: $\text{InCl}_3 \cdot 4\text{H}_2\text{O}$:TU of 1:2:0, 1:2:4 and 1:2:8 were made. The results show that 1:2:4 achieved the best device performance. (Fig. S8 and Table S3). The solution with 1:2:4 ratio was prepared as follow: first, 0.9713g thiourea (TU, 99%, Aladdin, recrystallized) was added into 10 mL DMF (99.8%, Bailingwei) under stirring to form a clear solution. Then, 1.8709g indium trichloride tetrahydrate ($\text{InCl}_3 \cdot 4\text{H}_2\text{O}$, 99.99%, Aladdin) and 2.2263g $[\text{Cu}(\text{NH}_2)_2\text{CS}_3]_2\text{SO}_4 \cdot \text{H}_2\text{O}$ were subsequently added to the above solution until completely dissolved. The precursor solution was filtered by a 0.80 μm polytetrafluoroethylene filter to obtain a clear DMF precursor solution (Fig. 2a).

The dimethylformamide (DMF) precursor solution with CuCl as precursor was prepared as follows: first, 2.4283g thiourea (TU, 99%, Aladdin, recrystallized) was added into 10 mL DMF (99.8%, Bailingwei) under stirring to form a clear solution. Then, 1.8709g indium trichloride tetrahydrate

Electronic Supplementary Material (ESI) for ChemComm.

($\text{InCl}_3 \cdot 4\text{H}_2\text{O}$, 99.99%, Aladdin) and 2.2263g CuCl were subsequently added to the above solution until completely dissolved. The precursor solution was filtered by a 0.80 μm polytetrafluoroethylene filter to obtain a clear DMF precursor solution.

Preparation of CISSe Absorber Films

Mo-coated soda-lime glass substrates were cleaned by sequential sonication in ultrapure water, acetone, and isopropanol, each for 15 min, and then dried under N_2 flow. The precursor solution was spin-coated on the substrates at a speed of 4000 rpm for 60 s. The wet films were immediately annealed on a hot plate at a temperature of 340°C for 90 s. The spin-coating and annealing were repeated for 12 times to reach the desired thickness. Then the films were put into a graphite box with Se tablets (0.35-0.38g) and placed in a tube furnace for selenization. The selenization was performed in a 0.16 Mpa Ar atmosphere and the selenization temperature was set at 630°C and the time was 17 min according to our previous report.^{1,2}

Fabrication of CISSe Solar Cells

After selenization, the absorber films were first etched in 14% $(\text{NH}_4)_2\text{S}$ solution for 15 min and then 50 nm CdS buffer layer was deposited on the top of the absorber by chemical bath deposition (CBD)^{3,4}. CBD was performed by loading the samples into a 65°C water bath beaker containing 22 mL 18.46 mmol/L CdSO_4 aqueous solution (99%, Sinopharm Chemical Reagent Co. Ltd.), 28 mL NH_4OH (25-28%, Sinopharm Chemical Reagent Co. Ltd.) and 150 mL ultrapure water under stirring. After stirred for 1 min, 22 mL 0.75 mol/L aqueous solution of TU (99%, Aladdin, recrystallized) was poured into the bath beaker and the solution was kept stirred for 15 min. A window layer containing 50 nm i-ZnO and 250 nm ITO were deposited on top of CdS by RF sputtering followed by thermal deposition of top contacts of nickel and aluminum (Ni/Al) through a shadow mask. The solar cell area was defined by mechanical scribing for approximately 0.10 cm^2 .

Elemental analysis

The analysis of elemental CHN was performed by Center of Materials Analysis, Nanjing University on the Vario MICRO Elemental Analyzer.

X-ray crystallography

Single-crystal X-ray diffraction of the complex were performed using a Bruker Smart Apex CCD diffractometer at room temperature with Mo- $K\alpha$ radiation ($\lambda = 0.71073 \text{ \AA}$). The program SAINT was used for integration of the diffraction profiles and an absorption correction was applied using the method of multi-scans. The structure was solved by direct methods using the SHELXS program of SHELXTL packages and refined anisotropically for all non-hydrogen atoms by full-matrix least squares on F^2 with the SHELXL program. All the hydrogen atoms were placed in geometrically calculated positions by using a riding model.⁵

Film and device characterization

X-ray diffraction (XRD) patterns (2θ scan) were collected by a Siemens D5005 X-ray powder diffraction system using Cu $K\alpha$ ($\lambda = 1.5406 \text{ \AA}$) X-ray as the source. The scan rate was 6 °/min.

Electronic Supplementary Material (ESI) for ChemComm.

The morphology of the films was measured on a Hitachi S4800 scanning electron microscope using 5 kV power. The elemental composition of the precursor film and CISSe absorption film was measured by energy dispersive X-ray spectroscopy (EDX). To avoid background signals from the substrate, which can distort the quantification of the elements by matrix effects, the measurement was performed at low acceleration voltages of 5 kV. The current density-voltage ($J-V$) curves of the CISSe solar cells were measured using a Keithley 2400 Source Meter under simulated AM 1.5 sunlight at 100 mW/cm^2 irradiance generated by an AAA sun simulator (CROWNTECH, Inc.). The intensity of the simulated sunlight was calibrated by an NREL calibrated Si reference cell. The external quantum efficiency (EQE) of the solar cells were measured on Enlitech QE-R3018 using calibrated Si and Ge diodes (Enli technology Co. Ltd.) as references.

Results and discussion

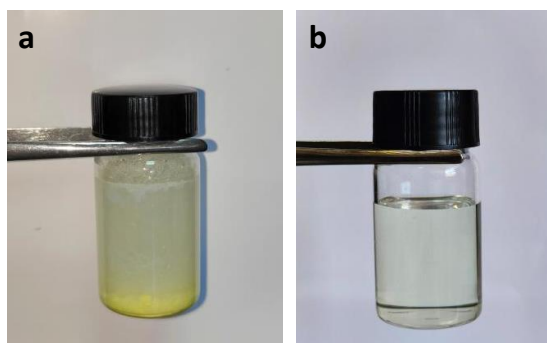


Fig. S1 Photos of solutions after reaction (a) and filtration (b).

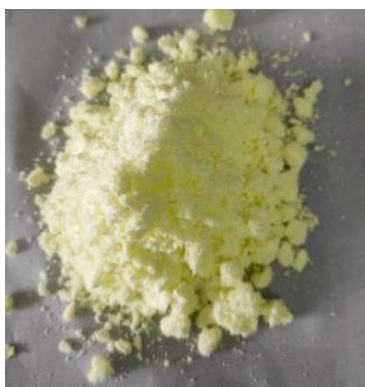


Fig. S2 Photograph of the pale yellow powder S1 obtained from solution in Fig. S1a.



Electronic Supplementary Material (ESI) for ChemComm.

Fig. S3 Photograph of the pH testing paper after dipped into the solution in Fig. S1b.



Fig. S4 Photograph of white crystals precipitated from the solution in Fig. S1b.



Fig. S5 Photograph of the white crystals (S2) obtained from Fig. S4.

In order to understand the composition of S1 and S2, we conducted a powder X-ray diffraction (XRD) analysis on S1 and S2. The results are shown in Fig. S6. The XRD patterns of S1 match perfectly with that of S₈. For S2, no matched compound was found.

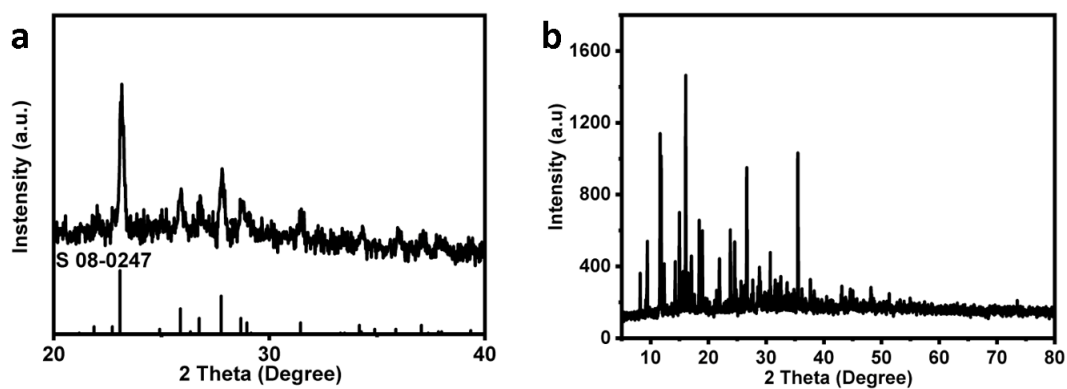


Fig. S6 XRD patterns of S1 (a) and S2 (b).

Electronic Supplementary Material (ESI) for ChemComm.

The report of the elemental analysis (CHN) of S2 is shown in Fig. S7. The measured and calculated contents of the C, H, and N elements based on $[\text{Cu}(\text{NH}_2)_2\text{CS}_3]_2\text{SO}_4 \cdot \text{H}_2\text{O}$ are summarized in Table S1. From Table S1, it can be seen that the measured contents of elemental C, H, and N are in perfect agreement with that calculated from the molecular formula of $[\text{Cu}(\text{NH}_2)_2\text{CS}_3]_2\text{SO}_4 \cdot \text{H}_2\text{O}$, confirming high purity of product S2.

国家教育部
STATE EDUCATION MINISTRY
南京大学现代分析中心
CENTER OF MATERIALS ANALYSIS, NANJING UNIVERSITY

检测报告

REPORT FOR DETECTING AND ANALYZING

委托单位: 南京邮电大学 (ENTRUSTING UNIT)	送样日期: 2022 年 2 月 22 日 (DATE OF SAMPLE SUPPLYING)
样品名称: $\text{Cu}(\text{CH}_3\text{COO})_2 \cdot \text{TH}$ 配合物 (SAMPLE NAME)	样品状态: 白色晶体 (SAMPLE STATE)
检测设备: Vario MICRO 元素分析仪 (INSTRUMENT)	检测项目: CHN 含量 (ITEMS FOR DETECTING AND ANALYZING)
检测依据: JY/T 0580-2020 元素分析仪分析方法通则 (BASIS FOR DETECTING)	

分析检测结果

RESULTS OF DETECTING AND ANALYZING

C%	H%	N%
10.42	3.54	22.59

(以下空白)

检测单位 (公章)
(DETECTING AND ANALYZING UNIT)

报告日期: 2022 年 2 月 23 日
(DATE OF REPORTING)

中心主任 (章)
(DIRECTOR)

本报告共 1 页, 其中图 0 页, 表 0 页。

说明:

1. 本报告检测项目为普通测试, 检测数据、结果和报告不具有任何证明作用, 仅供委托方参考。
2. 本报告涂改增删无效; 本报告不得部分复印, 本报告及其复印件未加盖本单位印章无效。
3. 委托检验仅对样品负责, 检测结果仅反映对所检样品的评价, 检测结果的使用、使用后产生的直接或间接损失, 检测方不承担任何责任。
4. 若对本报告有异议, 请于报告发出之日起 15 天内来本单位复检, 逾期不予受理。
5. 未经本中心同意, 任何单位或个人不得用本报告及本中心的名义作广告宣传。

地址: 中国南京汉口路 22 号
邮编: 210093
电话: (025)83592318

Center of Materials Analysis, Nanjing University
Hankou Road 22, Nanjing 210093, P.R. China
Tel: (025)83592318

Fig. S7 Report of the measurement and analysis of the CHN content of S2.

Table S1 The measured and calculated CHN contents of S2

Elements in S2	C	H	N	O	S	Cu
Measured mass percentage (%)	10.42	3.54	22.59	/	/	/
Calculated mass percentage (%) from [Cu((NH ₂) ₂ CS) ₃] ₂ SO ₄ ·H ₂ O	10.33	3.73	24.10	11.46	32.10	18.21

Table S2 Crystallographic data for [Cu((NH₂)₂CS)₃]₂SO₄ H₂O.

Formula	[Cu((NH ₂) ₂ CS) ₃] ₂ SO ₄ H ₂ O
Formula weight	697.89
Crystal system	orthorhombic
Space group	<i>Pbca</i>
<i>a</i> , Å	19.2009(11)
<i>b</i> , Å	12.3001(7)
<i>c</i> , Å	21.4316(13)
<i>α</i> , °	90
<i>β</i> , °	90
<i>γ</i> , °	90
<i>V</i> , Å ³	5061.6(5)
<i>Z</i>	8
<i>T</i> , K	297(2)
ρ_{calc} , g cm ⁻³	1.832
<i>F</i> (000)	2848
μ , mm ⁻¹	2.302
Index ranges	$-23 \leq h \leq 28, -17 \leq k \leq 18, -31 \leq l \leq 29$
θ range for data collection, °	2.691- 31.687
Measured reflections	8539
Independent reflections	5826
Data/restraints/parameters	8539/2/298
GOF (<i>F</i> ²)	1.006
<i>R</i> indexes [<i>I</i> > 2σ(<i>I</i>)]	<i>R</i> ₁ = 0.0376
	<i>wR</i> ₂ = 0.0656
<i>R</i> (all data)	<i>R</i> ₁ = 0.0752
	<i>wR</i> ₂ = 0.0753
$R_1 = \sum F_o - F_c / \sum F_o $; $wR_2 = [\sum w(F_o^2 - F_c^2)^2 / \sum w(F_o^2)^2]^{1/2}$	

Electronic Supplementary Material (ESI) for ChemComm.

To determine the optimal molar ratio, DMF precursor solutions with $[\text{Cu}(\text{NH}_2)_2\text{CS}_3]_2\text{SO}_4 \cdot \text{H}_2\text{O}:\text{InCl}_3 \cdot 4\text{H}_2\text{O}:\text{TU}$ of 1:2:0, 1:2:4 and 1:2:8 were prepared using the concentration of $\text{Cu}^+=0.638\text{mol/L}$ as a reference. The statistical device parameters and the $J-V$ curves of the best performing CISSe solar cells are shown in Fig. S8. The device parameters are summarized in Table S3. The results show a composition of 1:2:4 achieves the best device performance.

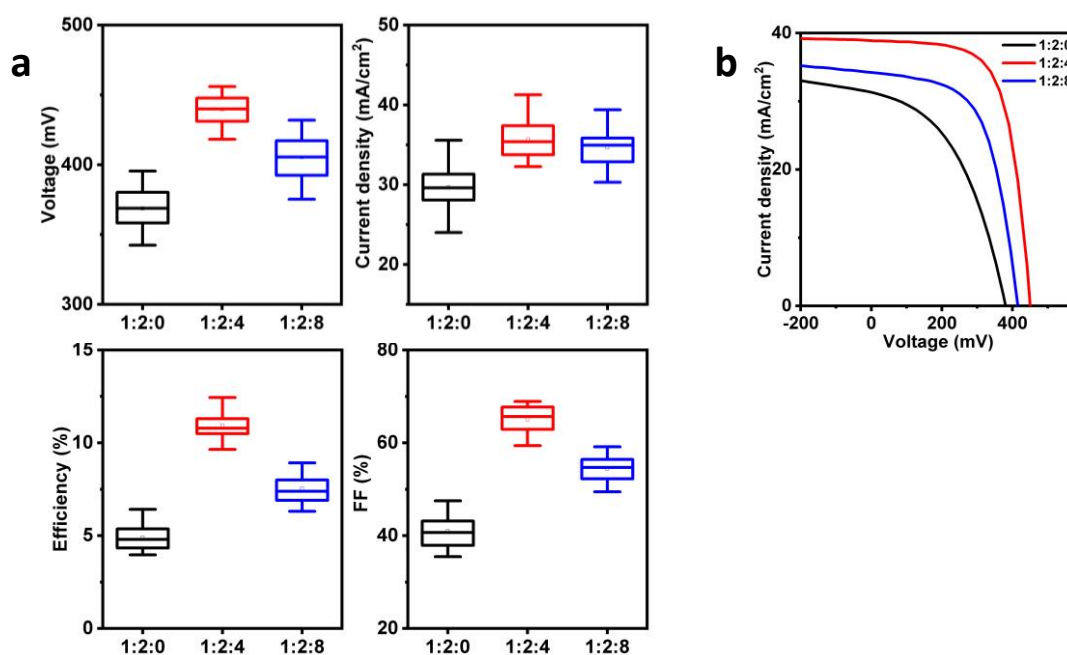


Fig. S8 (a) The statistical device parameters (a) and the $J-V$ curves (b) of the solar cells fabricated from solutions with $[\text{Cu}(\text{NH}_2)_2\text{CS}_3]_2\text{SO}_4 \cdot \text{H}_2\text{O}:\text{InCl}_3 \cdot 4\text{H}_2\text{O}:\text{TU}$ ratios of 1:2:0, 1:2:4 and 1:2:8.

Table S3 Summary of the device parameters of the best performing solar cells fabricated from solutions with $[\text{Cu}(\text{NH}_2)_2\text{CS}_3]_2\text{SO}_4 \cdot \text{H}_2\text{O}:\text{InCl}_3 \cdot 4\text{H}_2\text{O}:\text{TU}$ ratios of 1:2:0, 1:2:4 and 1:2:8..

Samples	V_{oc} (mV)	J_{sc} (mA/cm^2)	FF (%)	η (%)
1:2:0	393.4	31.30	52.15	6.42
1:2:4	450.1	38.90	66.35	11.62
1:2:8	415.4	34.23	59.28	8.43

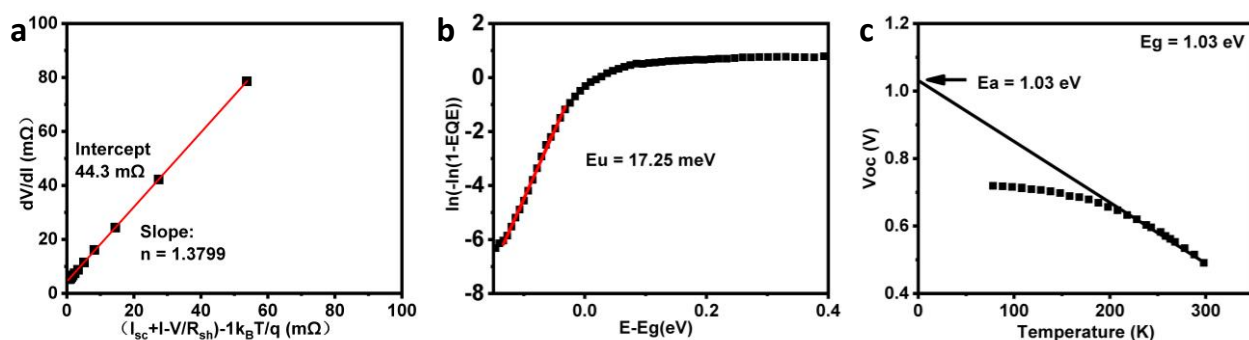


Fig. S9 (a) Extraction of the ideality factor (n) of the solar cell in Fig.2c. (b) Extraction of Urbach energy (E_U) from the EQE in Fig.2d. (c) Plots of the open-circuit voltage versus temperature (V_{OC} - T) and linear fit of activation energy (E_a) of the device in Fig.2c.

Table S4 Device parameters of the champion solar cell.

V_{oc} (V)	J_{sc} (mA/cm^2)	FF (%)	PCE (%)	EQE (%)	IQE (%)	n	J_0 (mA/cm^2)	E_g (eV)	E_a (eV)	E_U (meV)	R_s (Ω/cm^2)	R_{sh} (Ω/cm^2)
0.454	39.19	68.33	12.16	12.09	13.21	1.38	1.156×10^{-4}	1.032	1.030	17.25	14.31	12620

To compare the new complex to that without TU complexing, CISSe solar cells using CuCl as the copper source were fabricated in parallel to that of $[\text{Cu}(\text{NH}_2)_2\text{CS}_3]_2\text{SO}_4 \cdot \text{H}_2\text{O}$. The results are shown below in Figure S10 and Table S5. Device that uses CuCl as the copper source is marked as “CuCl” (black curves) and that use $[\text{Cu}(\text{NH}_2)_2\text{CS}_3]_2\text{SO}_4 \cdot \text{H}_2\text{O}$ as the copper source is marked as “[$\text{Cu}(\text{NH}_2)_2\text{CS}_3$] $_2\text{SO}_4 \cdot \text{H}_2\text{O}$ ” (red curves).

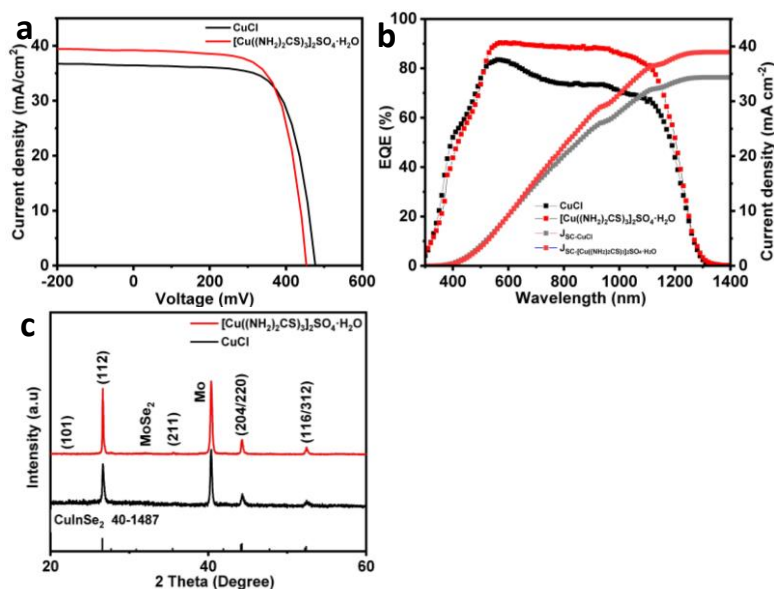


Figure S10 The J-V curves (a), EQE spectra (b), and the XRD patterns (c) of the CISSe devices (absorbers) respectively using CuCl (black curves) and “[$\text{Cu}(\text{NH}_2)_2\text{CS}_3$] $_2\text{SO}_4 \cdot \text{H}_2\text{O}$ ” (red curves) as Cu precursors.

Table S5 The device parameters of CISSe solar cells using CuCl and $[\text{Cu}(\text{NH}_2)_2\text{CS}_3]_2\text{SO}_4 \cdot \text{H}_2\text{O}$ as Cu precursor.

Cu precursor	V_{OC} (mV)	J_{SC} (mV/cm ²)	FF (%)	PCE (%)
CuCl	477.1	36.45 (34.37)	68.95	11.99 (11.31)
$[\text{Cu}(\text{NH}_2)_2\text{CS}_3]_2\text{SO}_4 \cdot \text{H}_2\text{O}$	454.0	39.19 (38.96)	68.33	12.16 (12.09)

In parentheses are the integrated J_{SC} from the EQE and PCE based on the integrated J_{SC} .

From the J - V curves (Fig. S10a) and EQE spectra (Fig. S10b), the device using $[\text{Cu}(\text{NH}_2)_2\text{CS}_3]_2\text{SO}_4 \cdot \text{H}_2\text{O}$ as copper source has higher J_{SC} with better EQE response in almost the whole absorption range of 500-1150 nm, comparable FF, and lower V_{OC} . The high J_{SC} indicates better absorber quality and less charge carrier recombination. The XRD patterns (Fig. S10c) demonstrate the CISSe absorber film using the new complex $[\text{Cu}(\text{NH}_2)_2\text{CS}_3]_2\text{SO}_4 \cdot \text{H}_2\text{O}$ as precursor has higher crystallinity, consistent with SEM image (Fig. 3c). The lower V_{OC} maybe due to unoptimized composition and selenization condition for this new complex system, which needs further investigation.

Table S6 Chemical composition of the precursor film and CISSe film.

Samples	Cu (Atomic %)	In (Atomic %)	S (Atomic %)	Se (Atomic %)	Cu/In
Precursor film	27.61	26.20	46.19	/	1.05
CISSe film	28.67	23.94	4.43	42.95	1.20

The elemental composition of the precursor film and CISSe film was determined by energy dispersive X-ray (EDX) analysis (Table S6). The Cu/In ratio is 1.00 in the precursor solution, similar to the precursor film (1.05). But the Cu/In ratio increased to 1.20 after selenization, much higher than 1.05, indicating a large loss of In during selenization. The results suggest that the precursor solution experiences minimal In loss during spin coating and thermal annealing. This may be attributed to the fact that $[\text{Cu}(\text{NH}_2)_2\text{CS}_3]_2\text{SO}_4 \cdot \text{H}_2\text{O}$ is coordinated with TU, which aids In complexation with TU and enhances the stability of the precursor solution. However, high-temperature selenization causes excessive In loss, resulting in a Cu-rich film. This highlights the importance of regulating In loss during selenization to control the CISSe/CIGSe composition and achieve highly performing CISSe/CIGSe thin film solar cells. We will investigate how to reduce the In loss in the subsequent study.

Reference

1. J. Jiang, S. Yu, Y. Gong, W. Yan, R. Zhang, S. Liu, W. Huang and H. Xin, *Solar RRL*, 2018, **2**, 1800044.
2. S. Wu, J. Jiang, S. Yu, Y. Gong, W. Yan, H. Xin and W. Huang, *Nano Energy*, 2019, **62**, 818-822.
3. H. Khallaf, I. O. Oladeji, G. Chai and L. Chow, *Thin Solid Films*, 2008, **516**, 7306-7312.
4. G. Brammertz, M. Buffière, Y. Mevel, Y. Ren, A. E. Zaghi, N. Lenaers, Y. Mols, C. Koeble, J. Vleugels, M. Meuris and J. Poortmans, *Applied Physics Letters*, 2013, **102**, 013902.
5. Y.-R. Su, K. Xiao, J.-W. Liu, F.-F. Ju, C.-Y. Qin, L.-Z. Wang, S. Wang and Y.-H. Li, *Journal of Chemical Research*, 2018, **42**, 77-79.